Switchable $Al_xGa_{1-x}As$ all-optical delay line at 1.55 μm

A. D. Bristow[a)]
Department of Physics and Institute for Optical Sciences, University of Toronto, 60 St. George Street, Toronto, Ontario M5S 1A7, Canada

R. Iyer and J. S. Aitchison
Department of Electronic and Computer Engineering and Institute for Optical Sciences, University of Toronto, 10 Kings College Road, Toronto, Ontario M5S 3G4, Canada

H. M. van Driel
Department of Physics and Institute for Optical Sciences, University of Toronto, 60 St. George Street, Toronto, Ontario M5S 1A7, Canada

Arthur L. Smirl
Laboratory for Photonics and Quantum Electronics, 138 IATL, University of Iowa, Iowa City, Iowa 52242

(Received 6 October 2006; accepted 17 January 2007; published online 7 March 2007)

The authors demonstrate an on-chip optical delay in $Al_xGa_{1-x}As$ that operates at room temperature and 1.55 μm. A nonlinear directional coupler for optical switching and a 188 ps long racetrack structure provide bit delays of >100 for picosecond pulses. In the linear regime the transmission ratio of the slow channel is 74%, which reduces to 40% with increasing peak intensity. (Meanwhile, the fast channel output increases from 26% to 60%.) Switching occurs due to a nonlinear detuning of the directional coupler, limited by three-photon absorption and time-averaging effects. This proof-of-principle device can operate at up to 5 GHz and is promising for optical buffering applications. © *2007 American Institute of Physics*. [DOI: 10.1063/1.2679838]

Control of the propagation time of light pulses in a medium is important in information technology and nonlinear optics. Recently, much attention has been devoted to schemes that exploit changes in the optical path length at a material resonance or by engineering photonic dispersions (Refs. 1–7 and references therein). Alternatively, optical delay lines can be created by simply increasing the physical path length in a device. This can be achieved in an optical fiber, producing large delays that are useful for buffering applications.[8–10]

Using semiconductor growth and fabrication technology, on-chip devices provide a platform for stable integrated architectures. Moreover, delay lines in $Al_xGa_{1-x}As$ can be constructed from routinely existing components such as waveguides, directional couplers, and optical switches. In this letter, we demonstrate a switchable all-optical delay line using a waveguide racetrack and a half-beat length nonlinear directional coupler (NLDC).[11,12] This on-chip device operates at room temperature and at telecommunication wavelengths, yielding a 188 ps delay between its undelayed path (fast channel) and delayed path (slow channel). In the linear regime the light preferentially travels through the slow channel. Increasing the peak intensity of the incident light switches the NLDC so that light predominantly exits the structure via the fast channel. This device is switched using the material nonlinearity, whereas the delay is determined by the geometry. It should be noted that we emphasize the application of the NLDC in a device that buffers light pulses rather than demonstrate an improved NLDC from previous work.[12]

Figure 1(a) shows a schematic of the all-optical delay line. The structure consists of a molecular beam epitaxially grown $Al_xGa_{1-x}As$ planar waveguide, which is etched to produce a straight waveguide (bus) and a racetrack delay line. Vertical optical confinement is obtained by a 1.5 μm $Al_{0.18}Ga_{0.82}As$ layer surrounded by $Al_{0.24}Ga_{0.76}As$ cladding layers (1.5 μm above and 4 μm below). The samples are patterned by photolithography and dry (reactive ion and inductively coupled plasma) etching. Key features of the fabrication are shown in scanning electron micrographs in Figs. 2(b) and 2(c). Each waveguide has an etch depth of approxi-

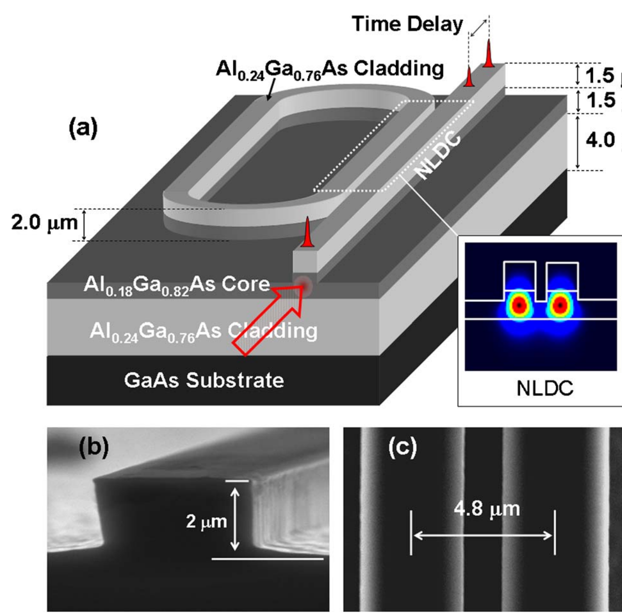

FIG. 1. (Color online) (a) Schematic diagram of the optical delay line structure and experimental geometry, showing the in-plane patterning of the bus waveguide, delay racetrack, and layer structure of the wafer. Also indicated is the NLDC, for which the cross section of the simulated supermode is shown in the inset. Scanning electron micrographs of the ridge waveguide cross section and the top view NLDCs are shown in (b) and (c), respectively.

[a)]Electronic mail: alan.bristow@utoronto.ca

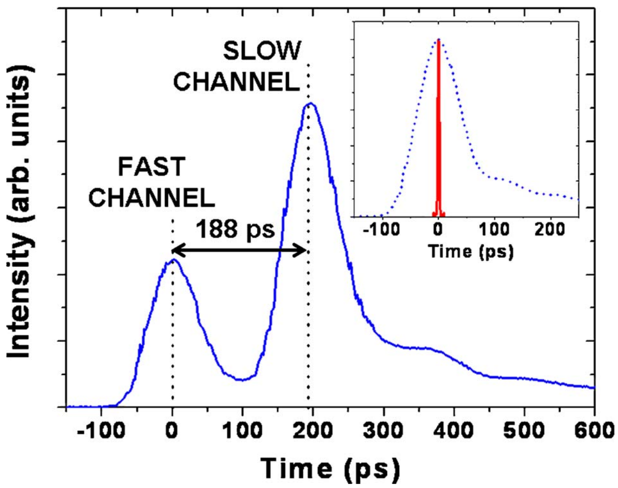

FIG. 2. (Color online) Temporal response of the linear transmission through the optical delay line for TE polarization measured with the fast photodetector. The inset shows the autocorrelation of the pulse from the OPO (solid red line) compared to the impulse response measured on the fast photodetector (dotted blue line).

mately 2 μm and a width of 3.5 μm. The NLDC has a coupling length of 2 mm and a waveguide center-to-center spacing of 4.8 μm. The racetrack waveguides have a bend radius of 2 mm and a round-trip time of 188 ps. A full vectorial finite-difference mode solver was used to design the structure. The individual sections (viz., straight waveguide, bent waveguide, and directional coupler) were optimized to find a converging set of parameters for the linear regime. In particular, the etch depth and bend radius were chosen to minimize the losses in the racetrack.

Optical experiments were performed with 1.7 ps pulses from a Ti:sapphire pumped optical parametric oscillator (OPO) at a repetition rate of 78.8 MHz. An autocorrelation trace of the OPO pulses is plotted in the inset of Fig. 2 (solid red line). The center wavelength of the pulses is $\lambda = 1.55$ μm, with a spectral width of approximately 2 nm. Pulses are attenuated using a $\lambda/2$ wave plate and a polarizing beam cube, which selects TE polarization to be launched into the cleaved facet of the chip via a microscope objective. The temporal response of the transmitted light is recorded by a 25 GHz InGaAs photodetector connected to a digital sampling scope, which is synchronized to the OPO repetition rate. Temporal resolution is limited to approximately 100 ps due to the detection electronics, and is clearly seen when comparing the impulse response of the photodetector (dotted blue line) to the autocorrelation of the OPO pulse in the inset of Fig. 2. This obscures the true bit delay, which is otherwise confirmed by cross correlation with idler pulses from the OPO (not shown here).

A pulse enters the structure and travels along the bus to the NLDC where, in the linear optical regime, it excites a supermode [see the inset of Fig. 1(a)] that allows light to evanescent couple between the bus and the racetrack. The pulse propagates around the racetrack returning to the NLDC where it couples back to the bus. The main part of Fig. 2 shows the temporal traces for TE polarization at low input peak intensity. The fast channel is used as a time marker, with the peak amplitude being arbitrarily chosen as 0 ps. The slow channel response dominates the trace and is centered at 188 ps, which corresponds to one round-trip of the racetrack (of modal and group indices of 3.26 and 3.42, respectively). The bit delay is >100, allowing a potential operation rate of at least 5 GHz (and more likely an order of magnitude higher). This device has a total linear loss (excluding insertion) of ~6 dB for TE polarized light in the slow channel.

Figure 3 shows the TE polarized temporal response of the all-optical delay line for a range of peak intensities inside the structure, after taking into account the 70% coupling efficiency and the 0.28 Fresnel reflection. As the peak intensity increases the overall signal amplitude increases in both channels. More interestingly, the dominant signal is exchanged from the slow channel (at low peak intensities) to the fast channel (at high peak intensities). This self-switching occurs all optically because the large nonlinear refractive index of the $Al_{0.18}Ga_{0.82}As$ ($n_2 = 1.5 \times 10^{-13}$ cm^2 W^{-1}) (Ref. 13) detunes the bus waveguide and inhibits the evanescent coupling to the racetrack.

The time traces are used to extract the amplitudes in each channel as a function of peak intensity. The raw data are corrected by a deconvolution to remove the impulse response of the photodiode; see the inset of Fig. 2. The fast channel (dashed blue line), slow channel (dot dashed red line), and total (solid black line) amplitudes are plotted in Fig. 4(a). All three curves increase with peak intensity and a crossing is observed between the fast and slow channels. The total amplitude increases linearly up to approximately 2 GW cm^{-2}, above which the gradient decreases due to strong nonlinear absorption. Since the experiments are performed below the half band gap of the $Al_{0.18}Ga_{0.82}As$ waveguide core layer, this is predominantly three-photon absorption. Furthermore, this effect occurs at intensities well above the onset of the nonlinear switching.

The switching properties are more clearly illustrated by plotting the transmission ratio of the fast (slow) channel ($T_{f(s)}$) as a function of peak intensity, as shown in Fig. 4(b). The transmission ratios are obtained by normalizing the amplitudes of the individual channels against the total; thus, $T_{f(s)} = A_{f(s)}/(A_f + A_s)$, where $A_{f(s)}$ is the amplitude of the fast (slow) channel, shown in Fig. 4(a). In the linear regime the transmission ratios of the fast and slow channels are 26% and 74%, respectively. This corresponds to an ~91% one-way coupling efficiency in the NLDC after the linear loss and the length of the two paths are considered. While there are no physical limits to half-beat length NLDCs with 100% cou-

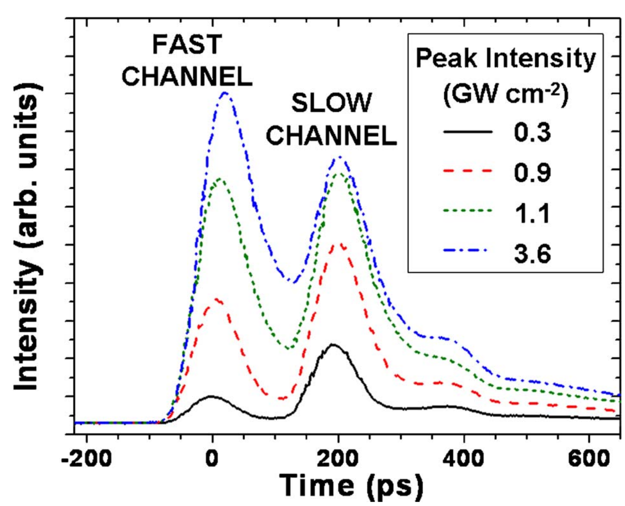

FIG. 3. (Color online) Temporal traces for TE polarized transmission through the optical delay line for several incident peak intensities.

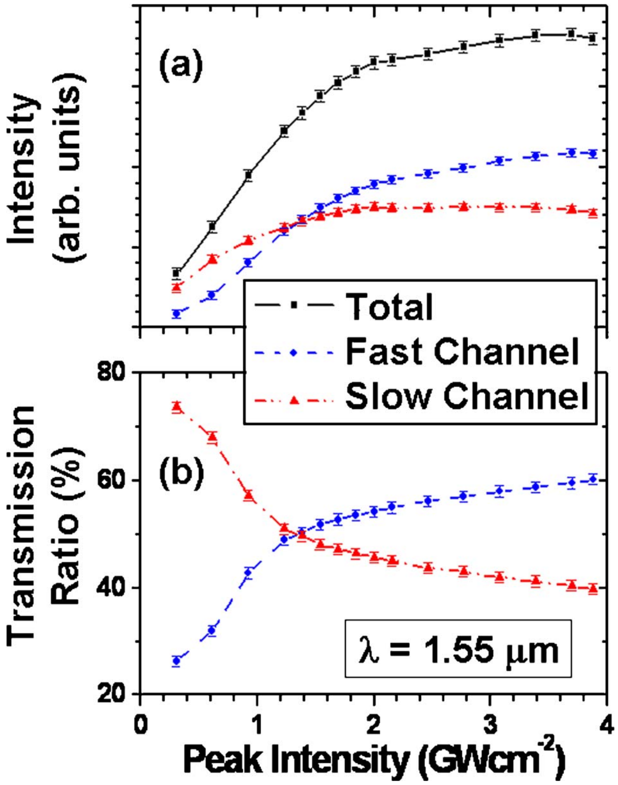

FIG. 4. (Color online) (a) Peak amplitude for pulses in the fast channel (dashed blue line), the slow channel (dash dotted red line), and the total (solid black line) as a function of the incident peak intensity. (b) Transmission ratio for the fast and slow channels is plotted as a function of peak intensity.

pling in the linear regime, the value we obtained is sufficient for demonstration purposes. A 50% switching occurs at approximately 1.4 GW cm^{-2}, above which the transmission ratio of the fast and slow channels flatten out at 60% and 40%, respectively. At these high peak intensities the two ratios do not completely invert (compared to the values in the linear regime) due to the observed nonlinear absorption and time-averaging effects, whereby the wings of the pulse continue to traverse the slow channel.[12] Time-averaging effects can be minimized by modifying the input pulses, for example, by using either square pulses[14] or solitons.[15] Further improvements can be achieved by altering the band gap of the waveguide core with respect to the wavelength of operation, which has been supported by preliminary data for different excitation wavelengths on this device.

At higher peak intensities, the exiting pulse shape is unclear from the above experiments. For comparison, the linear and nonlinear transmissions of a 2 mm long section of a straight waveguide cleaved from this structure were examined using an optical spectrum analyzer. At the onset of the nonlinear absorption (discussed above), the observed self-phase modulation corresponds to a nonlinear phase shift of $\sim 1.5\pi$. These results agree well with numerical simulations of the self-phase modulation and with expectations from the literature.[12]

In summary, an all-optical $Al_xGa_{1-x}As$ racetrack delay line is demonstrated at room temperature with 1.55 μm light pulses. This proof-of-principle device has a bit delay of >100 that can be operated at 5 GHz, and it can simultaneously buffer up to ~ 50 bits. The delay can be switched off by nonlinear optical interactions in the coupling region, which can attain a <15 dB switching ratio by engineering the material absorption and the length of the nonlinear directional coupler. Furthermore, the on-chip nature of this device allows its integration into more complex architectures.

The authors would like to thank J. E. Sipe, P. Chak, and Z. S. Yang for interesting and fruitful discussions. This work was funded by the Defence Advanced Research Projects Agency and the Natural Sciences and Engineering Research Council of Canada.

[1] D. J. Gauthier, A. L. Gaeta, and R. W. Boyd, Photonics Spectra **44**, 40 (2006).
[2] Y. A. Vlasov, M. O'Boyle, H. F. Hamann, and S. J. McNab, Nature (London) **65**, 438 (2005).
[3] H. Gersen, T. J. Karle, R. J. P. Engelen, W. Bogaerts, J. P. Korterik, N. F. van Hulst, T. F. Krauss, and L. Kuipers, Phys. Rev. Lett. **94**, 123901 (2005).
[4] Q. Xu, S. Sandhu, M. L. Povinelli, J. Shakya, S. Fan, and M. Lipson, Phys. Rev. Lett. **96**, 123901 (2006).
[5] Z. Deng, D.-K. Qing, P. Hemmer, C. H. R. Ooi, M. S. Zubairy, and M. O. Scully, Phys. Rev. Lett. **96**, 023602 (2006).
[6] J. B. Khurgin, J. Opt. Soc. Am. B **22**, 1062 (2005).
[7] G. Lenz, B. J. Eggleton, C. K. Madsen, and R. E. Slusher, IEEE J. Quantum Electron. **37**, 525 (2001).
[8] R. Langenhorst, M. Eiselt, W. Pieper, G. Grosskopf, R. Ludwig, L. Kuller, E. Dietrich, and H. G. Weber, J. Lightwave Technol. **14**, 324 (1996).
[9] W. De Zhong and R. S. Tucker, J. Lightwave Technol. **16**, 1737 (1998).
[10] T. Sakamoto, K. Noguchi, R. Sato, A. Okada, Y. Sakai, and M. Matsuoka, Electron. Lett. **37**, 454 (2001).
[11] J. S. Aitchison, A. H. Kean, C. N. Ironside, A. Villeneuve, and G. I. Stegeman, Electron. Lett. **27**, 1709 (1991).
[12] A. Villeneuve, C. C. Yang, P. G. J. Wigley, G. I. Stegeman, J. S. Aitchison, and C. N. Ironside, Appl. Phys. Lett. **61**, 147 (1992).
[13] J. S. Aitchison, D. C. Hutchings, J. U. Kang, G. I. Stegeman, and A. Villeneuve, IEEE J. Quantum Electron. **33**, 341 (1997).
[14] A. M. Weiner, Y. Silberberg, H. Fouckhardt, D. E. Leaird, M. A. Saifi, M. J. Andrejco, and P. W. Smith, IEEE J. Quantum Electron. **25**, 2648 (1989).
[15] N. J. Doran and D. Wood, J. Opt. Soc. Am. B **4**, 1843 (1987).